

On the hemispheric origins of meltwater pulse 1a

W.R. Peltier*

Department of Physics, University of Toronto, 60 St. George Street, Toronto, Ontario, M5S 1A7, Canada

Received 5 November 2003; accepted 7 June 2004

Abstract

During the glacial–interglacial transition that began subsequent to the Last Glacial Maximum approximately 21,000 calendar years ago, globally averaged (eustatic) sea-level rose by approximately 120 m as climate warmed to its current (Holocene) state. This rise of relative sea-level (RSL) did not occur smoothly, however, but was characterized by the occurrence of one or more episodes of extremely rapid increase. The most extreme of these events has come to be referred to as meltwater pulse 1a, and was initially identified in the coral based record of RSL history from the island of Barbados in the Caribbean Sea. Although it has usually been assumed that this episode of rapid RSL rise was derivative of a partial collapse of the northern hemisphere ice sheets, it has recently been suggested that this pulse could have originated in a dramatic melt-back of the Antarctic Ice Sheet. In this paper the arguments presented in favour of the southern hemisphere source are revisited in order to assess the plausibility of this alternative scenario.

Based upon the analyses presented, it is concluded that the evidence previously provided in support of the southern hemisphere scenario is in fact unable to rule out an entirely northern hemisphere source for the meltwater pulse 1a. Since explicit evidence does exist that both the Laurentide and Fennoscandian ice sheets contributed to this event and that Antarctic ice sheet melting occurred significantly later, the southern hemisphere appears not to have been a prime mover of northern hemisphere events.

© 2005 Elsevier Ltd. All rights reserved.

1. Introduction

The issue as to the geographic source(s) of the meltwater that entered the ocean basins during the meltwater pulse 1a event originally identified by Fairbanks (1989), hereafter MWP1a, is clearly important, both from the perspective of the climate dynamics underlying the deglaciation process itself, and from the perspective of the geophysical response of the solid Earth to the removal of ice from the continents. If more ice were to have been removed from one continent rather than another, then the ongoing response in terms of relative sea-level (RSL) history would be expected to be more intense on the continent from which the greater amount of ice were removed. Insofar as RSL histories measured at sites remote from the main concentrations

of LGM land ice are concerned, however, it is an interesting issue as to whether it is possible to uniquely infer the geographical source of the meltwater responsible for a particular episode of rapid sea-level rise on the basis of such data.

Very recently (Clarke et al., 2002), it has been suggested that simultaneous observations of the strength of MWP1a at Barbados (Fairbanks, 1989; Bard et al., 1990) and at the Sunda Shelf (Hanebuth et al., 2000) might be employed to rule out a northern hemisphere source for this event. Somewhat prior to the appearance of the paper by Clarke et al. (2002), however, RSL history predictions for both the Sunda Shelf and Barbados locations were published in Peltier (2002a) based upon computations performed using the ICE-4G (VM2) model of Peltier (1994, 1996), a model in which an MWP1a event had been built into the ICE-4G deglaciation history in order that a good fit to the Barbados record could be achieved. The assumption

*Tel.: +1 416 978 2938; fax: +1 416 978 8905.

E-mail address: peltier@atmosph.physics.utoronto.ca.

made in constructing the ICE-4G model of deglaciation was that the entire MWP1a event originated in the northern hemisphere. Fig. 1 presents a reproduction of the fit of the ICE-4G (VM2) model prediction of postglacial relative sea-level rise at Barbados to the Barbados observations. The amplitude of MWP1a in the ICE-4G model, which is evident by inspection of the step-discontinuous eustatic sea-level history shown together with the smooth sea-level curve predicted by the theory, is approximately equal to 25 m, an amplitude which Clarke et al. (2002) accept as a good estimate. Evident by further inspection of Fig. 1 (based upon Fig. 3 of Peltier, 2002a), is that MWP1a has been introduced in the model at precisely 14,000 calendar years before present. In the smooth dashed curve that represents the theoretically predicted RSL history, however, the smoothing effected by the coarse (1 kyr) temporal resolution of the model is such that the modelled MWP1a is somewhat reduced in amplitude (by 3–4 m). Inspection of Figs. 4 and 7 in Peltier (2002a) will show that the amplitudes of MWP1a at Barbados and the Sunda Shelf are within a few metres of one another, a result that may be in conflict with the conclusions of Clarke et al. (2002) that a northern hemisphere source might lead to such a large difference in the amplitude of MWP1a at Barbados and the Sunda Shelf that such a geographic source could be ruled out. On this basis the authors are led to surmise that MWP1a may have originated from the southern hemisphere and therefore from the Antarctic continent. This logic is interesting and deserves to be further explored. This is the purpose of the present paper. My approach will be to perform a new series of relative sea-level history predictions using the ICE-4G (VM2) model of the deglaciation process in order to compute the expected differential amplitude of MWP1a between Barbados and the Sunda Shelf. I will also consider the modifications to these predictions that follow from application of the newly published ICE-5G (VM2) model of Peltier (2004). It will also be of interest to consider the physical processes that are most responsible for controlling the differential amplitudes predicted by these different models. Of primary concern, however, will be the issue as to whether the uncertainties in the data are such as to enable the differential amplitude predictions to be useful as a means of determining the geographical region from which meltwater was derived.

Prior to proceeding with this investigation, it will be important to situate MWP1a with respect to the most important changes in surface climate that are known to have occurred during the glacial–interglacial transition in the time since Last Glacial Maximum (LGM). To this end, Fig. 2 intercompares the $\delta^{18}\text{O}$ data from the GRIP and GISP2 deep ice-cores from Summit Greenland, an atmospheric temperature proxy, the Barbados sea-level curve, and the atmospheric temperature record from the Vostok, Antarctica ice core. Also shown in this figure is

the range of time that is conventionally taken to correspond to Heinrich event 1 (H1), as well as the range of time corresponding to MWP1a. All of these data are shown over the range of time from 8000 calendar years ago to 18,000 calendar years ago. Inspection of the data shown in Figs. 1 and 2 will show that there is no resolvable RSL rise during H1, although a significant rise associated with it cannot be ruled out as there is a gap in the data from Barbados during this interval of time (see Hemming, 2004 for detailed discussion). Meltwater pulse 1a, on the other hand, clearly begins essentially simultaneously with the onset of the Bølling warm period at approximately 14,200 calendar years ago. As the northern hemisphere warms, evidenced by the $\delta^{18}\text{O}$ data from the GRIP and GISP2 cores, a very large amplitude pulse of fresh water is applied to the ocean basins. Since this intense northern hemisphere warming finds essentially no expression in the southern hemisphere temperature record from Vostok, Antarctica, it would seem reasonable to expect that the water of MWP1a must have had a northern hemisphere source. This expectation is further reinforced by inspection of Fig. 3, where I show the rate of change of sea level based upon the Barbados record together with the summer seasonal insolation at 60°N latitude, the orbital forcing to which the northern hemisphere ice sheets were subjected during the glacial interglacial transition. Clearly evident by inspection of this figure is the fact that both MWP1a and the weaker MWP1b (Fairbanks, 1989) that occurred at the end of the Younger-Dryas cool period (centred upon 12,000 calendar years), occurred during the summer seasonal insolation maximum. During the same period, of course, the southern hemisphere was experiencing a summer seasonal insolation deficit, a circumstance that is clearly not conducive to any significant instability of the Antarctic ice-sheet. These arguments are all suggestive of the notion that MWP1a may have been sourced primarily in the northern hemisphere.

The idea that it could have been sourced in the southern hemisphere derives from the notion, to be further discussed in the concluding section of this paper, that the addition of meltwater to the surface of the southern ocean would have caused the process of Antarctic Deep and Intermediate water production to decrease and thereby caused the process of North Atlantic deepwater (NADW) formation to intensify, thus warming the Northern Hemisphere. However, an alternative interpretation appears to be equally viable, namely that the collapse of the North Atlantic THC triggered by Heinrich event 1 (H1) was followed by a spontaneous reactivation of the NADW production process after the meltwater loading of the North Atlantic associated with H1 ceased. That NADW production did collapse following H1 is clearly demonstrated by the time series of the Pa/Th kinematic tracer

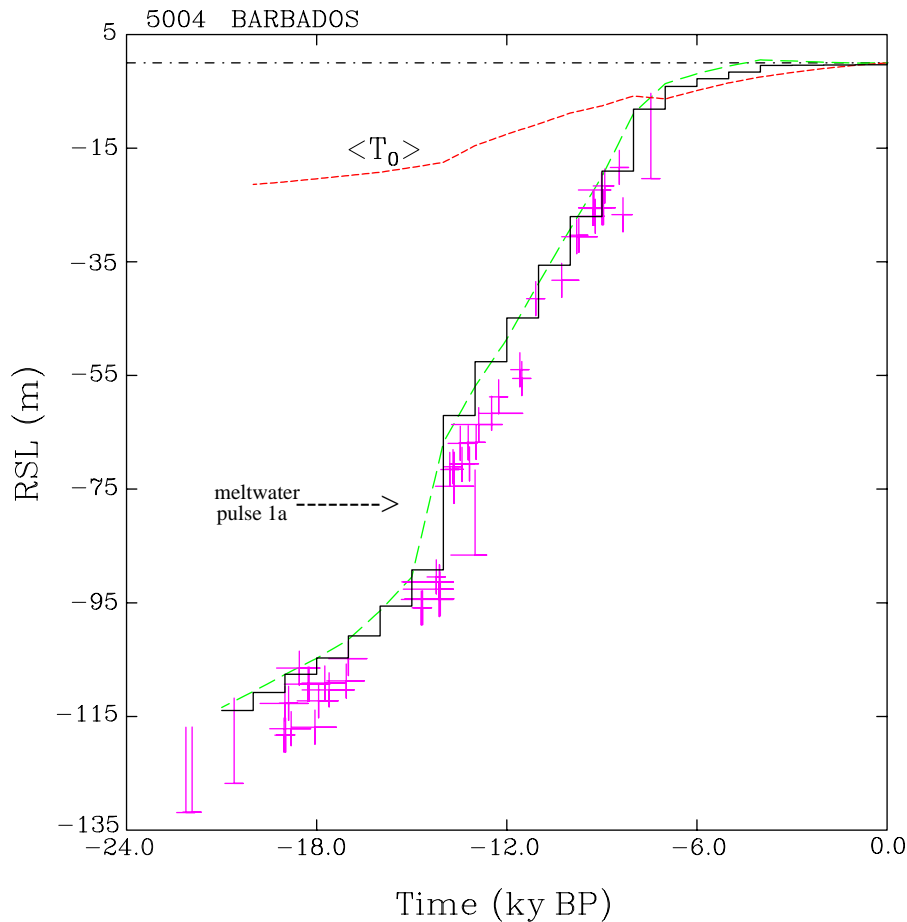


Fig. 1. The coral based record of relative sea level history from the island of Barbados in the Caribbean Sea as presented in Fairbanks (1989) on the U/Th based timescale of Bard et al. (1990). The crosses are observations based upon the *Acropora Palmata* (Ap) species of corals with the vertical segment of the cross corresponding to the depth range of 5 m below sea level that the Ap species may extend. The long vertical bars with cross-bar positioned at the actual depth at which the sample was found are data based upon the *Porities* species of coral which may live at great depth below sea level. The step discontinuous black curve is the eustatic function of the model based upon the amount of ice melted at each 1 kyr spaced time step of the model, including both explicit and “implicit” ice (see Peltier, 1998 for a discussion of the implicit component). The smooth green curve is the predicted RSL history at Barbados obtained by solving (1) using the ICE-4G model of deglaciation history but neglecting the influence of rotational feedback, neglecting the influence of the “broad shelf effect” (Peltier and Drummond, 2002) and assuming that the continental ice sheets that were in place at LGM were in isostatic equilibrium with the underlying Earth. The curve denoted $\langle T_0 \rangle$ in this figure is that denoted $\Delta\Phi(t)/g$ in Eq. (1) in the text to follow.

of the strength of the Atlantic MOC recently published by McManus et al. (2004). That it would spontaneously re-invigorate under the action of the wind driven circulation once the freshwater forcing due to iceberg discharge ceased is entirely expected.

The argument in Clarke et al. (2002) for an Antarctic source begins with the idea of sea-level “fingerprinting” as discussed in Mitrovica et al. (2001). These authors had addressed the question as to whether, on the basis of modern tide-gauge observations of the ongoing rate of global sea-level rise, it might be possible to identify the source(s) of any ongoing eustatic rise by exploiting the differences between the rates of RSL rise observed at different geographic locations. This idea had in fact been introduced many years earlier by Clark and Lingle (1977) who had already computed

the nature of the geographically non-uniform RSL rise signal that would be an expected consequence of melting of the West Antarctic ice sheet. Similarly, Clark (1976) had already commented upon the fact that adjacent to a continental region from which land ice was melting, sea level would be expected to rise much less rapidly than elsewhere as a consequence of the action of self-gravitation. This results from the fact that sea level adjacent to the continental ice mass is held anomalously high by the direct effect of the gravitation attraction of the ice, an effect that has been included in the theory of postglacial RSL history since the work of Clark et al. (1978) and Peltier et al. (1978). Clark et al. (2003) have recently published a reminder of these earliest calculations of the “fingerprints” of global sea level rise.

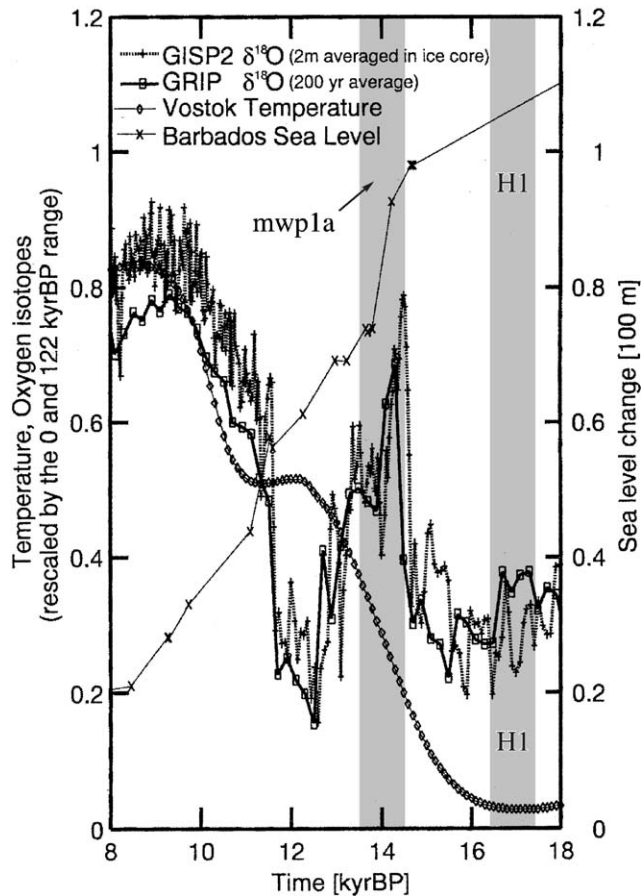


Fig. 2. Proxy records of climate variability between 8 kyr BP and 18 kyr BP. The Greenland temperature proxies, i.e. oxygen isotope records from the GRIP and GISP2 deep ice cores are normalized by their maximum deviation between 0 and 122 kyr BP. The temperature record from Vostok, Antarctica is also normalized by its range between 0 and 122 kyr BP. The Barbados sea level record over this range of time is represented as a function of a nominal range of 100 m. Also shown on this Figure by the hatched regions are the ranges of time over which MWP1a and Heinrich event 1 occurred.

In Clarke et al. (2002), the idea of using measurements of RSL rise from different geographical regions to “fingerprint” the geographical source of the meltwater responsible for the observed RSL rise was extended to the analysis of paleo-recordings, specifically those mentioned previously from Barbados and the Sunda Shelf, of the amplitude of MWP1a. Computations presented in that paper were based upon the assumption that MWP1a was produced by instantaneous melting from a number of distinct plausible northern hemisphere and/or southern hemisphere locations. In analyzing the data it was assumed that the amplitude of sea-level rise that should be produced at six distant locations, including the Sunda Shelf and Barbados, could be accurately predicted on the basis of the ansatz that the distribution of water over the ocean basins could be determined by computing the distribution that occurred “elastically”. That is, the continuing redistribution of

water due to previous melting and the visco-elastic relaxation of the Earth that accompanied earlier deglaciation could also be neglected. Subject to this reasonable assumption and to the assumption that MWP1a was sourced from a particular location or locations, these authors computed (see their Fig. 2) the MWP1a sea-level change expected at a number of locations, including Barbados and the Sunda Shelf, the only locations at which MWP1a is actually recorded. Their analyses delivered a much smaller amplitude of MWP1a at Barbados than on the Sunda Shelf when MWP1a was sourced in the Laurentide ice sheet. Since MWP1a was assumed by these authors to have approximately the same amplitude at Barbados and the Sunda Shelf, the authors concluded that a northern hemisphere source was incompatible with the observations (see their Fig. 2). It is a significant issue, however, as to the quality of the constraint upon the amplitude of MWP1a that is available either from Barbados or from the Sunda Shelf, as we will see in what follows.

The purpose of this paper will be to discuss in some detail why it is that the ICE-4G (VM2) scenario of Peltier (2002a) or the refined ICE-5G (VM2) scenario of Peltier (2004) is able to fit the MWP1a amplitude observations even though all of the meltwater is sourced from the northern hemisphere, thereby implying that these observations cannot be construed to argue that any significant portion of MWP1a originated in Antarctica. Although these models, in which no contribution to MWP1a comes from Antarctica, should be viewed as end member models, exercising them will enable us to test the utility of the Clarke et al. (2002) method of “fingerprinting” the source of sea-level rise as a means of inferring the geographical origins of the meltwater added to the oceans.

2. Theory of postglacial sea-level change

The mathematical methods that have been developed to predict the variations of relative sea-level rise forced by a given scenario of continental deglaciation were established in papers published in the 1970s (Peltier, 1974, 1976; Peltier and Andrews, 1976; Farrell and Clark, 1976; Clark et al., 1978; Peltier et al., 1978). Since these initial papers were published, the theory has been further embellished through extensions that enable it to predict the impacts upon planetary rotation due to the glaciation–deglaciation process (Peltier, 1982; Wu and Peltier, 1984) and to enable it to incorporate the influence of the time dependent variations in the coastline (Peltier, 1994, 1996). The theory is also being employed to predict the horizontal motions forced by deglaciation (James and Morgan, 1990; James and Lambert, 1993; Mitrovica et al., 1994; Peltier, 1994), measurements of which are now being made using

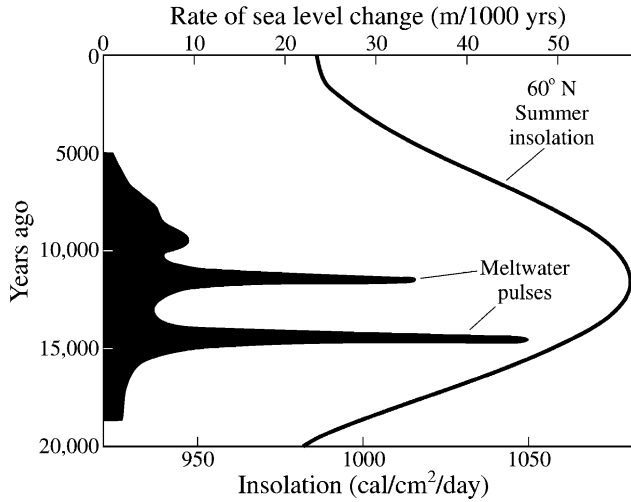


Fig. 3. Illustrates the time dependent rate of influx of meltwater into the oceans based upon the computation of the time derivative of the relative sea level curve of Fairbanks (1989) on the timescale of Bard et al. (1990). Also shown is the solar insolation curve for summer at 60°N latitude.

space-geodetic methods (Argus et al., 1999; Milne et al., 2001). It has also been possible to extend the theory so as to enable it to calculate the strength of the feedback of the changing rotation upon sea level itself (e.g. see Peltier, 1998, 2002b for a discussion of the form of the theory that is consistent with that employed to compute the change in the rotational state). In the near future we will be able to further exercise the theory by employing it to predict the time dependence of geoid height globally that will be measured by the recently launched GRACE satellite system (Peltier, 1999, 2002b; Douglas and Peltier, 2002; Peltier, 2004). It will be useful for the reader of this paper to know that the software being employed by Mitrovica et al. (2001) and Clarke et al. (2002) to compute the “fingerprints” of various sea level rise scenarios is that of Peltier (1974 and subsequent) with an additional subroutine based upon the application of a spectral method to solve the sea level equation (SLE, see below) presented originally in Mitrovica and Peltier (1991).

The basic structure of this theory is contained in an equation that I have come to call the Sea Level Equation (SLE), in which the space and time dependent history of RSL change induced by an assumed known model of continental glaciation and deglaciation, say $S(\theta, \lambda, t)$, is given by

$$S(\theta, \lambda, t) = C(\theta, \lambda, t) \left[\int_{-\infty}^t dt' \int_{\Omega} d\Omega' \{ G^L(r - r', t - t') \times L(r, t) + G^T(r - r', t - t') T(r', t') \} + \Delta\Phi(t)/g \right]. \quad (1)$$

In (1) the surface load $L(r', t)$ has the following composite form involving the densities of ice and water, respectively ρ_I and ρ_w , and the ice thickness I and relative sea level S :

$$L(\theta, \lambda, t) = \rho_I I(\theta, \lambda, t) + \rho_w S(\theta, \lambda, t). \quad (2)$$

Since the relative sea-level history $S(\theta, \lambda, t)$ appears not only on the left-hand side of (1), but also under the triple convolution integral, this equation is clearly an integral equation. The functions G^L and G^T in (1) are Green functions for the surface mass loading and tidal potential loading problems respectively (see Peltier, 2002b for details), whereas the function T is the variation of the centrifugal potential caused by the changing rotational state of the planet due to the direct effect of the surface mass load forcing. Since this effect of rotational feedback will be of interest in the present context, it will prove useful to state the form of T explicitly, as

$$T(\theta, \lambda, t) = T_{00} Y_{00}(\theta, \lambda) + \sum_{m=-1}^{+1} T_{2m} Y_{2m}(\theta, \lambda), \quad (3)$$

where

$$T_{00} = \frac{2}{3} \omega_3(t) \Omega_o a^2, \quad (4a)$$

$$T_{20} = \frac{1}{3} \omega_3(t) \Omega_o a^2, \quad (4b)$$

$$T_{2,+1} = (\omega_1(t) - \omega_2(t)) (\Omega_o a^2 / 2) \sqrt{2/15}, \quad (4c)$$

$$T_{2,-1} = -(\omega_1(t) + i\omega_2(t)) (\Omega_o a^2 / 2) \sqrt{2/15}. \quad (4d)$$

In Eqs. (4) the $\omega_i(t)$ are the variations in the individual Cartesian components of the angular velocity vector of the planet which are computed, for a given model of surface deglaciation and internal visco-elastic structure of the planet, using the theory of Peltier (1982) and Wu and Peltier (1984). The expressions (4) are those required in the expansion (3) that is based upon the assumption that this must include only terms that are of first order in the angular velocity perturbations $\omega_i(t)$. As pointed out in Peltier (1998, 1999), this linearization is required in order that the expression for T be compatible with the theory being employed to compute the $\omega_i(t)$. The derivation of the expressions (4) follows the original analysis of Dahlen (1976) whose work was performed in the context of an entirely different problem.

Crucial to the accurate solution of the SLE (1) is the method employed to compute the function $\Delta\Phi(t)$ which must be introduced so as to ensure that the glaciation-deglaciation process conserves mass. Since the ocean

function $C(\theta, \lambda, t)$ is time dependent (this function is zero over the continents and unity over the oceans) due to coastline migration, the construction of the time series $\Delta\Phi(t)$ requires careful attention to detail. Since this aspect of the theory will also be important in the present context it will be useful to provide this detail explicitly. A succinct description follows by first re-writing (1) schematically as

$$S(\theta, \lambda, t) = V(\theta, \lambda, t) + D(t), \quad (5)$$

from which the multiplicative factor C has been eliminated because the field S is defined everywhere over the surface of the planet, even where there is no ocean. Considered in this way, $S(\theta, \lambda, t)$ is simply the perturbation of the height of the geoid (the surface of constant gravitational potential that is coincident with the surface of the sea where ocean exists) relative to the surface of the solid Earth. Now Eq. (1), and thus (5), is solved discretely in time using the iterative procedure described in Peltier (1998a). Suppose that we consider the change in sea-level between the $(n-1)$ st time step and the n th time step. If $C_n = C_{n-1}$, then the change in the thickness of the water load at a given point on the surface, and thus relative sea level, would simply be $(S_n - S_{n-1})C_n$. However, if $C_n \neq C_{n-1}$ then the change in water load will not be accurately estimated by this expression at those locations where C_n differs from C_{n-1} because of coastline migration.

There are two primary sources of error that arise due to the time dependence of C , namely a source that exists within the interior of the zone where initially glaciated regions later become inundated by the sea, and a source in those locations outside the zones of glaciation in which, for example, initially exposed continental shelf is being inundated by the sea due to the melting of continental ice. Both of these sources of error were first explicitly recognized in Peltier (1998a). In previous work on the influence of time dependent ocean function, these two regions have been treated separately. In particular, the interior region has been addressed by accounting for the action of “implicit ice” (Peltier, 1998b) and the exterior region has been dealt with by recognizing the influence of a “broad shelf effect” (Peltier and Drummond, 2002).

In a modified version of the algorithm to be employed for some of the analyses of this problem herein, the interior and exterior regions in which C varies are treated simply by storing knowledge of the increment in relative sea-level S_{n-1} , obtained in the previous time-step in the iterative solution of Eq. (1) as well as the form of the ocean function C_{n-1} , and paleotopography (Peltier, 1994) that obtained at the same time (this increases the machine memory required to perform the computations but increases accuracy. We then compute the actual sea-level change in the regions of changing C , using expressions that respect the volume of the ocean

lost or gained between the evolving paleotopography and the equipotential surface of the sea, as:

- (A) Outside the region of glacial unloading, the actual increment in water load is (broad shelf effect):

$$\Delta S_n^1 = -(S_n - S_{n-1} + T_n)(C_n - C_{n-1})C_n \quad (6a)$$

for $S_n > S_{n-1}$ (deglaciation).

- (B) Inside the region of glacial unloading, the change in the water load is (Previously dealt with by introducing the concept of implicit ice):

$$\Delta S_n^2 = T_{n-1}(C_{n-1} - C_n)C_{n-1} \quad (6b)$$

for $S_n < S_{n-1}$ (deglaciation).

In these expressions T_{n-1} and T_n are the paleotopographies at the $n-1$ st and n th time steps respectively, with the paleotopography as defined in Peltier (1994) such that it is negative over the water covered regions (during the glaciation phase of the cycle these expressions must be modified in the obvious way). Since our analyses with the new ICE-5G (VM2) model will include the influence of a full cycle of glaciation and deglaciation, there will be no contribution to sea level history from implicit ice of type I as defined in Peltier (1998), whereas the requirement that account continue to be taken of implicit ice of type II remains. The latter circumstance will be understood to obtain because, in considering the variation of sea-level through a cycle of glaciation and deglaciation, we assume for the sake of simplicity (as in previous work) that the distribution of land ice remains equal to the LGM distribution throughout the glaciation phase of the cycle (in particular regions like Hudson Bay are assumed to be ice covered immediately that the cycle begins). The “broad shelf effect” is fully captured in Eq. (6a) as previously.

The final step in the analysis is to compute the increment in the mass conservation term $D(t)$ between consecutive time steps. This follows from knowledge of the change in the water load at every point in space between the $n-1$ st and the n th time step, as

$$\Delta S_n = (S_n - S_{n-1}) + \Delta S_n^1 + \Delta S_n^2. \quad (7)$$

Multiplying this by the density of sea water and integrating over the entire surface of the Earth, the result must be equal to the mass of ice that was lost from (gained by in the glaciation phase of the cycle) the continents; thus from Eq. (1) we have:

$$D_n \langle C_n \rangle = D_{n-1} \langle C_n \rangle - \langle (V_n - V_{n-1})C_n \rangle - \langle \Delta S_n^1 \rangle - \langle \Delta S_n^2 \rangle + \frac{\rho_I}{\rho_w} \langle \Delta I_n \rangle \quad (8)$$

Given initial conditions, $D_o, V_o = 0$ we may compute D_1 and thus accumulate $(D_1 + D_2 + \dots)$ to obtain the

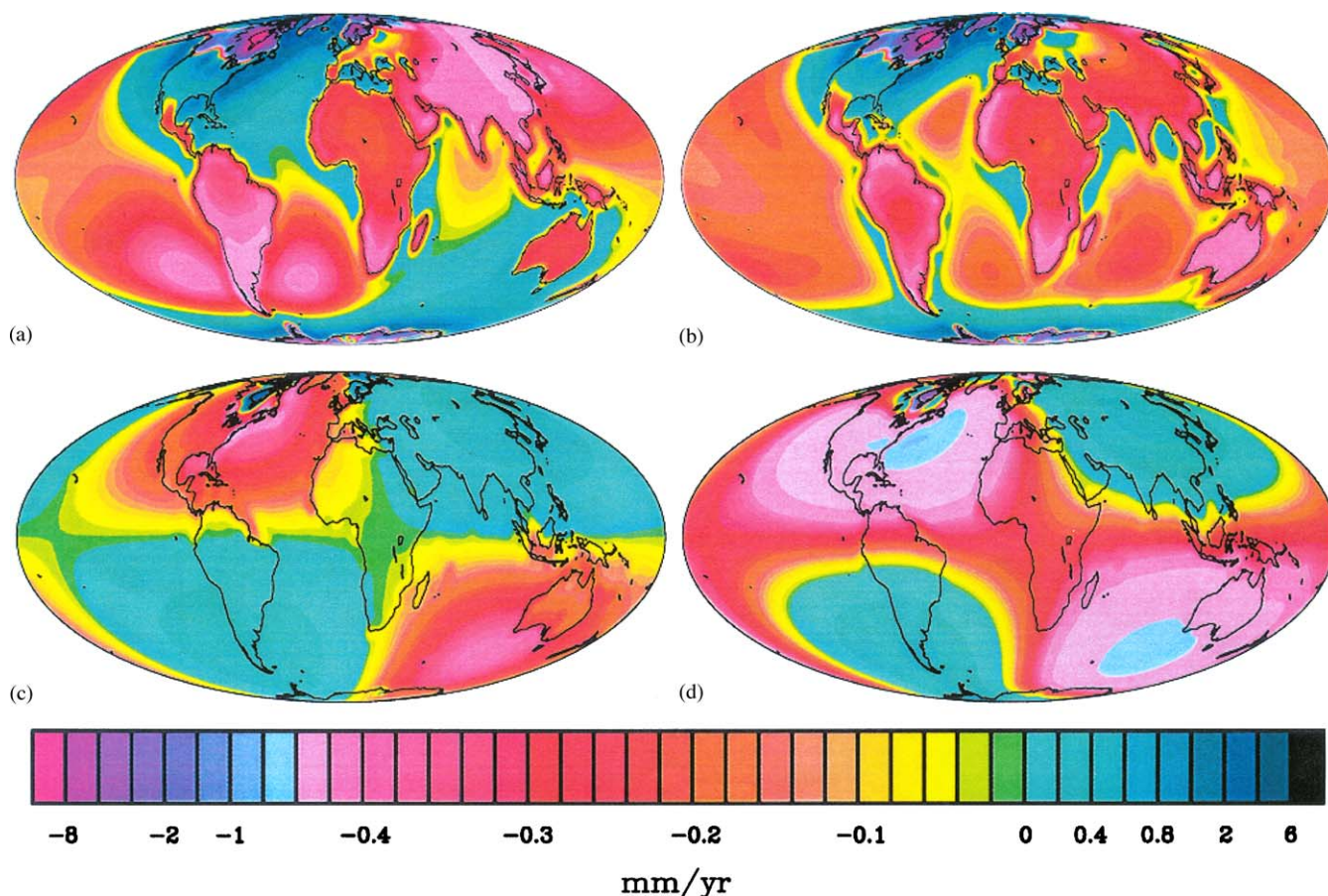


Fig. 4. An example of the solution for postglacial RSL history obtained by solving Eq. (1) employing the ICE-4G model of continental deglaciation and the VM2 model of the radial viscoelastic structure. In parts (a) and (b) of this Figure are shown predictions of the present day rate of RSL change both including (a) and excluding (b) the influence of rotational feedback. Plate (c) shows the difference between the prediction (a) and (b) (as a-b), demonstrating that the influence of rotational feedback is dominated by the influence of polar motion as it has the form of a spherical harmonic of degree 2 and order 1 (see Eqs. (4)). Part (d) of the figure shows the sum of the present day predicted rate of relative sea level rise from (a) and the theoretically predicted rate of increase of the radius of the solid Earth based upon a computation performed using the mathematical expression in Eq. (8a) of Peltier (2002b). This field is simply the field of geoid height time dependence due to the glacial isostatic adjustment process. This field is currently being measured using the GRACE satellite system.

complete time history of the mass conservation correction $\Delta\Phi(t)/g$ in (1).

As an initial demonstration of the results that we continue to produce based upon the application of the theoretical structure embodied in Eq. (1), I show in Fig. 4 model predictions of the present day rate of sea level rise both including (a) and excluding (b) the influence of rotational feedback. The difference in these two fields, shown in (c), has the form of a spherical in 2 and order 1 indicating that this effect is dominated by the motion of the rotation pole forced by the glacial isostatic adjustment process. This is evident on the basis of Eqs. (4c) and (4d) which demonstrate that the $T_{2,-1}$ and $T_{2,+1}$ terms in (3) depend entirely upon $\omega_1(t)$ and $\omega_2(t)$, which are the angular velocity perturbations that determined the motion of the pole. In part (d) of Fig. 4 I show the sum of the result shown in part (a) and the model predicted rate of radial displacement with respect to the

center of mass. This field is therefore the model predicted rate of change of geoid height measured with respect to the center of mass. This is precisely the measure of gravity field time dependence that will be observed by the GRACE satellite system. In the Results section to follow we will show that the dominant contribution to the differential amplitude of MWP1a at Barbados and on the Sunda Shelf derives from the influence of rotational feedback. However, as we will also show, this differential effect remains sufficiently small as to be unresolvable by the available RSL data from these two regions.

3. Results

As discussed in the Introduction to this paper, the model of MWP1a that is embodied in the ICE-4G deglaciation history of Peltier (1994, 1996) is one which

Contributions to MWP1a

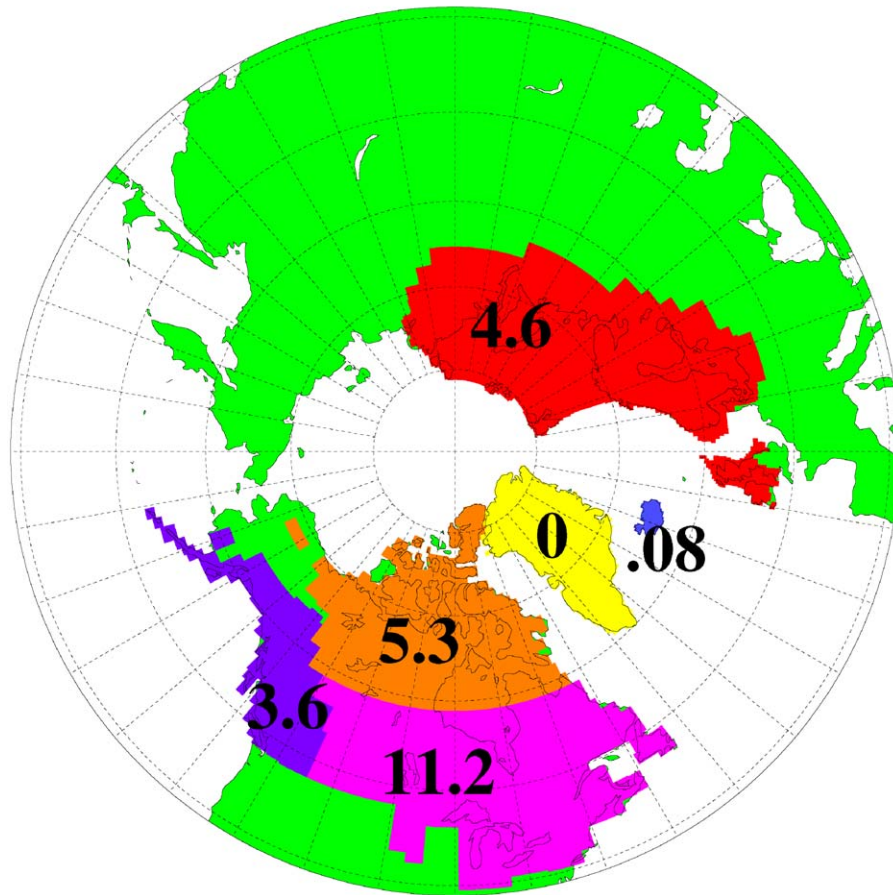


Fig. 5. Polar projection of the distribution of continental ice at Last Glacial Maximum and of the contribution from each of the primary sectors of the land ice distribution to the approximately 25 m eustatic rise of sea level that occurred during MWP1a.

appears to deliver predictions of the amplitude of this event at Barbados and on the Sunda Shelf that are not sufficiently different so as to enable the difference to be employed to determine the geographical source(s) of the meltwater responsible for this episode of rapid sea level rise (Peltier, 2002a). One reason for this may have to do with the distributed nature of the northern hemisphere source assumed in the ICE-4G model. This is illustrated in Fig. 5 where I show, in north polar projection, the contribution to MWP1a, in meters of eustatic sea level rise, that is assumed to emanate from North America and Northwestern Europe in this model. This characteristic of the ICE-4G deglaciation model has not been described previously. Adding these contributions together it will be noted that the sum is 24.8 m, essentially the same as the amplitude of MWP1a that is usually assumed to be recorded at Barbados and shown previously in Fig. 1. Also illustrated in Fig. 1 is the fact that the meltwater from each of these regions in the ICE-4G model is assumed to be removed instantaneously at 14,000 calendar years before present.

Of primary interest here is clearly the relative amplitude of the MWP1a event caused by the simultaneous addition of the meltwater from all of these regions at the Barbados and Sunda Shelf locations. The results of this initial comparison are shown in Fig. 6 for the ICE-4G model. In this figure I am showing the results for these two regions for four different “flavours” of the theoretical calculation. The first of these, labelled simply VM2, is for a calculation in which it is assumed that the ICE-4G LGM ice-thickness distribution is in isostatic equilibrium, in which the “broad shelf effect” is neglected and in which rotational feedback is also ignored. Also shown are results that include the contribution due to the “broad shelf effect” as recently described by Peltier and Drummond (2002), namely that labeled VM2+S. The result labelled VM2+P, on the other hand, is for a computation that includes the influence of the history of loading and unloading of all ice sheets prior to LGM, and therefore incorporates the specific degree of isostatic disequilibrium at LGM that is predicted using the VM2 model of the

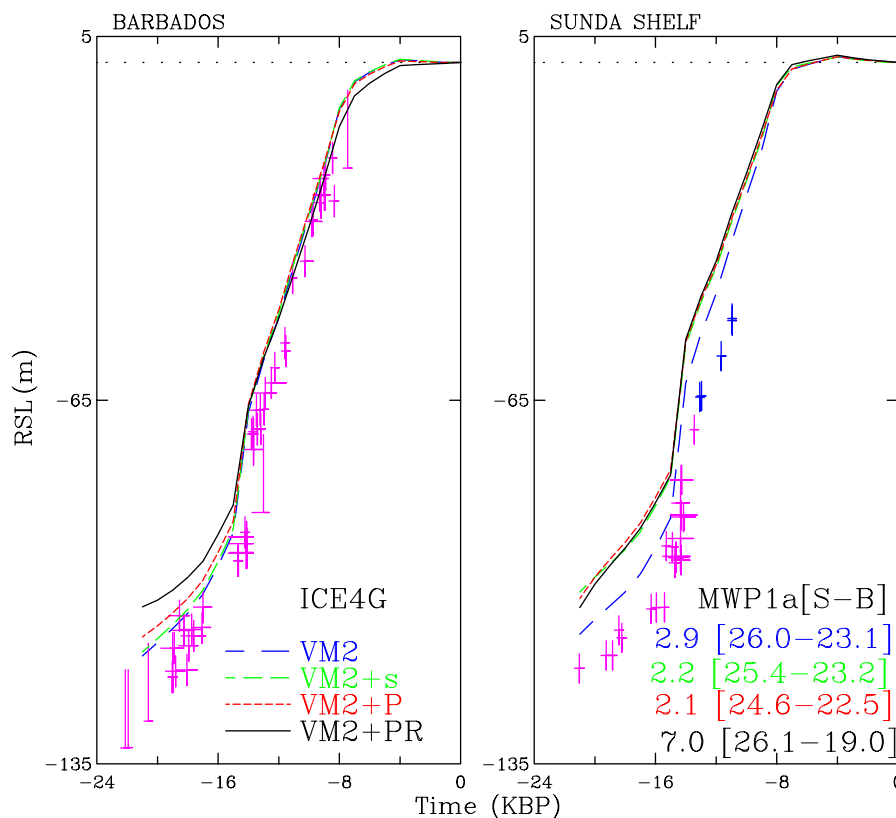


Fig. 6. RSL history predictions for Barbados and the Sunda Shelf for four different flavors of the theoretical computation based upon the use of the ICE-4G deglaciation model and the VM2 model of the radial viscoelastic structure. The curve denoted VM2 neglects the “broad shelf effect”, the history of glaciations and deglaciation prior to LGM, and the influence of rotational feedback. The shelf effect alone is included in VM2+S, the influence of prehistory alone in VM2+P, and both prehistory and rotational feedback VM2+PR. In the Sunda Shelf frame of the Figure are shown the differential amplitudes of MWP1a between the Sunda Shelf and Barbados for each of these flavors of the computation.

internal viscoelastic structure. The final curve, labeled VM2+PR, includes not only the influence of glaciation prehistory but also the influence of rotational feedback. Notable by inspection of this complete suite of analyses is that this version of the ICE-4G model has somewhat too little ice since the most accurate of the analyses, that labeled VM2+PR, lies above the sea level index points at greatest age (this point has been previously discussed in Peltier, 2002b). It is important to note that the version of ICE-4G being employed here is the same as that employed in Peltier (2002a) which is characterized by an eustatic rise of only 113.5m. In spite of this global mass deficiency we may still compare the amplitude of MWP1a at these two locations, given an eustatic input of 24.8m at 14,000 years before present, and these comparisons are listed on the Sunda Shelf portion of the figure. Inspection will show that, for the VM2, VM2+S, VM2+P, and VM2+PR predictions respectively, the amplitude of MWP1a at the Sunda Shelf exceeds that at Barbados by 2.9, 2.2, 2.1 and 7.0m, respectively. Even the largest of these differences, namely that for VM2+PR, is less than the largest differential amplitude of MWP1a between these sites,

computed using the assumptions in Clarke et al. (2002), by almost a factor of 2. The error bars on the data from these two locations are such that a differential amplitude of this magnitude provides no basis upon which to infer the geographical source of MWP1a. This fact will be discussed in greater detail in the concluding section of this paper. It is however the case that theory predicts the amplitude of the pulse at Sunda Shelf to be greater than that at Barbados, a results that is in accord with the analysis reported in Clarke et al. (2002) in regards to the sign of the differential amplitude.

It is nevertheless clear, on the basis of inspection of Fig. 6, that insufficiently much ice has been removed from the continents in ICE-4G to satisfy the observations. In order to investigate the extent to which this flaw in the model may be contributing to an underestimation of the differential effect, Fig. 7 shows the same analysis as in Fig. 6 but using the modified model denoted ICE-5G (Peltier, 2004). This model differs from ICE-4G primarily in that a significant increase in ice-mass has been added over the Canadian Prairies in order to eliminate the misfits of the ICE-4G (VM2) model to

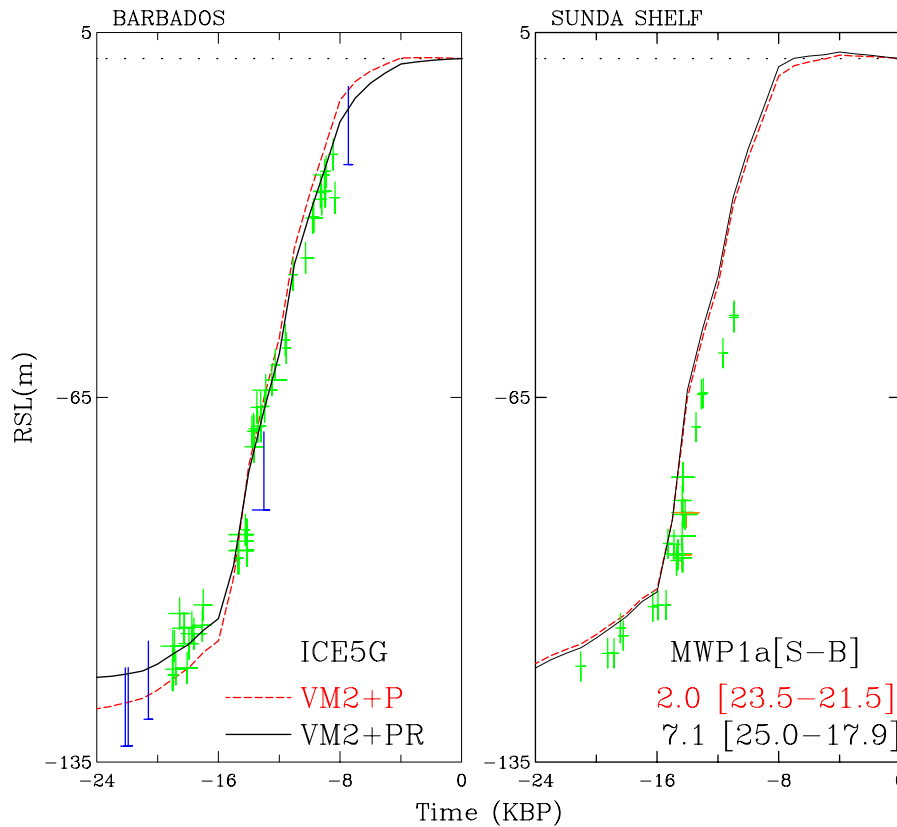


Fig. 7. Same as Fig. 6 but for the ICE-5GP model of deglaciation discussed in Peltier (2002b). This model differs from ICE-4G in that additional ice mass has been added over the Canadian Prairies in order to eliminate misfits to absolute gravity and VLBI data that otherwise exist. See Peltier (2002b) for a detailed discussion of this alternative model. Insofar as the various contributions to MWP1a are concerned, these are identical to those shown in Fig. 5.

the vertical motion of the solid Earth observed at the Yellowknife location that has been documented by Argus et al. (1999), as well as the misfits to the absolute gravity data recently compiled by Lambert et al. (2001) at a sequence of stations extending from Churchill on the west coast of Hudson Bay southwards across the US-Canada border into Iowa. A detailed discussion of the ICE-5G model and of the extent to which it is able to eliminate these misfits has been provided recently in Peltier (2004).

Inspection of the intercomparisons in Fig. 7 shows that for this modified model, the computations for which were performed using the modified computational procedure outlined in Eqs. 6a,b–8 the differential amplitudes of MWP1a between the Sunda Shelf and Barbados are now 2.0 and 7.1 respectively, for computations of type VM2+P, and VM2+PR. Once more the amplitude of MWP1a at the Sunda Shelf is, for both flavors of the calculation, greater than that at Barbados, as is the case in the calculations reported in Clarke et al. (2002). However, once more the maximum differential amplitude is too small, given the error bars on the observations, to enable us to come to any robust conclusion concerning the geographical origin of

MWP1a. A full discussion of these error bars will be provided in what follows.

It is notable on the basis of these two analyses of the predicted differential amplitude of the MWP1a event, that the largest differences between Barbados and the Sunda Shelf are induced by the influence of rotational feedback. It is therefore an entirely legitimate question as to whether the strength of the influence of rotational feedback upon sea level history is accurately accounted for in the models that we have elected to analyse. Although it is well known that the ICE-4G (VM2) model delivers an accurate prediction of both of the anomalies in Earth rotation associated with the glacial isostatic adjustment process (non-tidal acceleration and true polar wander, see Peltier, 1998), since the fit of the model to these anomalies is employed to fix the viscosity in the lowermost mantle, it is not at all clear that the feedback of changes in Earth rotation onto sea level itself will also be acceptable. No previous analysis save the initial investigation reported in Peltier (2002b) has investigated this issue. The question will be further investigated in what follows in order to determine whether error in the computation of this influence might be responsible for our underestimating the differential



Fig. 8. Location map for all South American sites for which data is available in the University of Toronto archive including those for which comparisons between RSL observations and theoretical predictions are shown in Fig. 9.

amplitude of MWP1a between Barbados and the Sunda Shelf.

In order to be certain that the influence of rotational feedback onto sea level history is approximated with sufficient accuracy in the previously described results, it proves useful to focus upon a geographical region in which the influence on Earth rotation due to the GIA effect is optimally strong. Returning to consideration of Fig. 4(c), it will be clear that it is along the southeast coast of South America, in Argentinian Patagonia, where the degree 2 and order 1 pattern associated with the feedback of Earth rotation upon sea level is of largest amplitude. This is furthermore a region that is sufficiently remote from the main centers of continental deglaciation that the influence of rotational feedback should be easiest to discern. Relative sea level observations from this region, and for much of the east coast of South America, have recently been compiled in Rostami et al. (2000) and we will focus upon the comparison of

these data with predictions of the ICE-4G (VM2) model prediction in order to provide an assessment of the extent to which these intercomparisons may provide further confidence in the strength of the feedback effect that is embodied in the model. To this end Fig. 9 shows a sequence of 8 intercomparisons between theory and observations at named sites ranging from the coast of Venezuela in the north to Tierra del Fuego in the south, the individual locations of which are shown in Fig. 8. A discussion of data sources will be found in Rostami et al. (2000) (Fig. 9).

Inspection of these intercomparisons, which are shown once more for a set of four different flavours of the theoretical calculation similar to those employed in the analyses shown in Fig. 6, leads immediately to a number of interesting and important conclusions. Prior to discussing these, one should note that the four different ICE-4G calculations for each site, here labeled “standard ICE-4G dash-dot (blue)”, “+shelf effect dashed (red)”, “+prehistory dashed (magenta)” and “+rotation (black)”, represent a sequence in which the radial viscosity structure is fixed to VM2 and the three different subtle effects are successively added such that it is only for the model labeled “+rotation (black)” in which the influence of rotational feedback onto sea level history is included. Beginning with the inspection of the theoretical model fits to the data at the sites in Venezuela and northern Brazil, it will be clear that all of the model predictions are very close to one-another. It is, nevertheless, interesting to note that at the Venezuela sites which lie north of the equator, the theoretical prediction that includes the influence of rotational feedback lies below all of the other curves. For sites that lie south of the equator, for example Recife, Brazil, on the other hand, the theoretical prediction that includes rotational feedback lies above the predictions made by models that exclude this effect. This is entirely expected based upon the results shown in Fig. 4c on which the influence of rotational feedback upon RSL history is isolated so as to reveal its degree 2 and order 1 form. On a traverse that crosses the equator from north to south, the sign of the impact of rotational feedback upon the predicted present day rate of RSL rise changes.

Moving to sites located progressively further south along the east coast of the South American continent, such as those in southern Brazil and northern Argentina, we eventually begin to encounter locations at which the observed height of the mid-Holocene highstand reaches altitudes above mean sea level of 5–6 m. At such sites only the model that includes the influence of rotational feedback onto sea level actually fits the observations. Rostami et al. (2000) have drawn attention to the fact that the amplitude of the mid-Holocene highstand along this coast increases systematically from north to south. Fig. 10 shows the predicted southwards

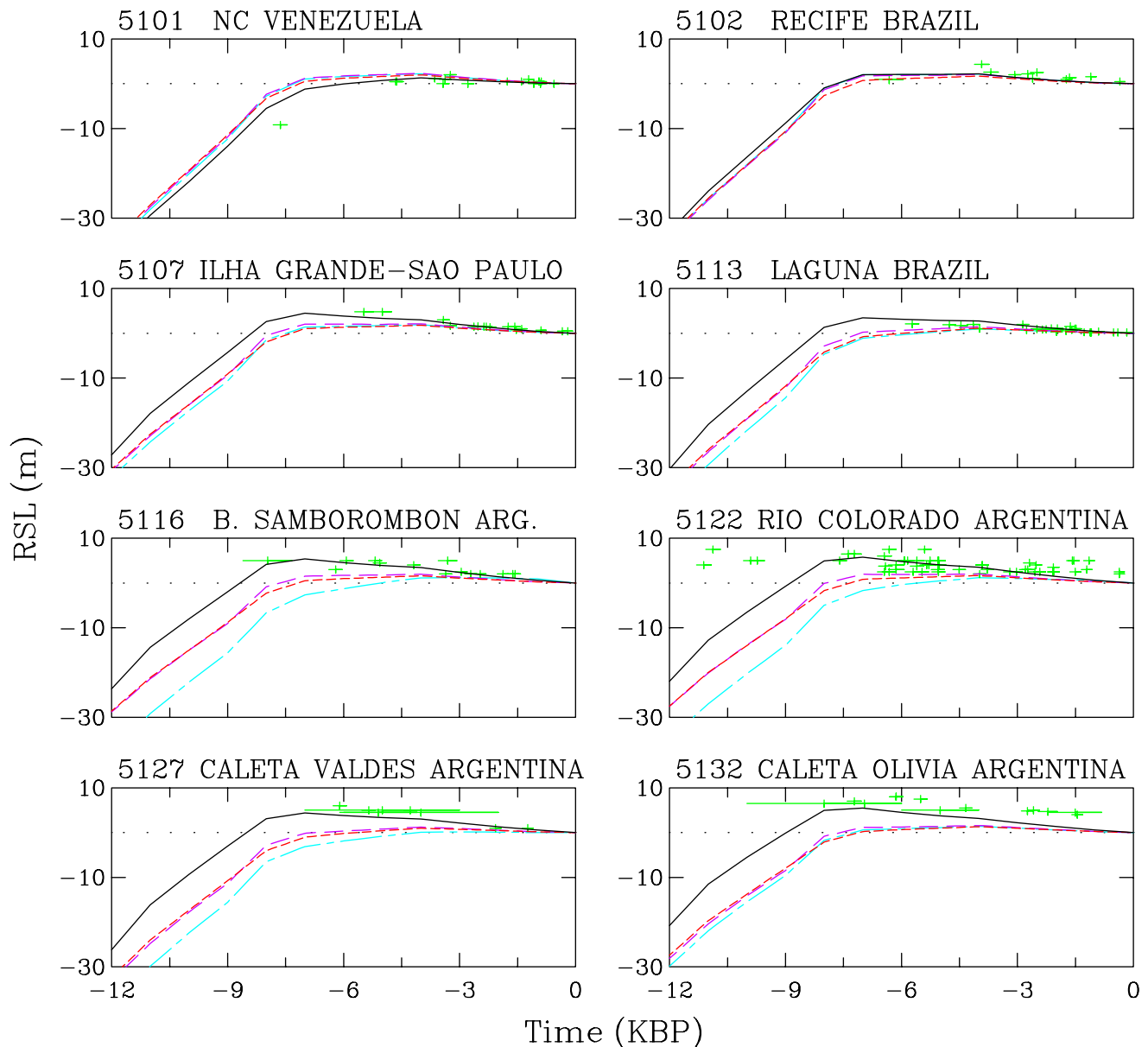


Fig. 9. Model-data relative sea level intercomparisons for 8 sites along the east coast of Argentinian Patagonia. Theoretical calculations are shown for four different variants of the theory. That labeled ICE-4G includes neither adjustment for the “broad-shelf effect”, glaciation prehistory or rotational feedback. These special effects are added one-at-a-time for the additional calculations shown. The last two digits of the numbers adjacent to the place names are the same as those employed to designate locations on the site map shown in Fig. 8.

slope of the highstand according to the ICE-4G (VM2) model, intercomparisons of which with the observed slope shown in Fig. 11 of Rostami et al. (2000) will show that this characteristic of the observations is also well reproduced by the theoretical model. It is very important to note, however, that the mid-Holocene highstand at the sites from which we have data does not increase smoothly as a function of increasing latitude to the south of the equator. This is a consequence of the fact that the coastline is rather irregular, resulting in the superposition of longitude dependent effects upon the more smoothly varying influence of rotational feedback.

Given the reasonably good fits to the highstand observations along the coast only when rotational feedback is included in the calculation, we are in a good position to argue that the strength of the influence of rotational feedback onto sea level that is embodied in the ICE-4G (VM2) model is rather accurate and therefore that our estimates of the maximum differential amplitude of MWP1a at Barbados and the Sunda Shelf is also accurate.

It is worthwhile commenting at this point on the extent to which our results are discrepant from those reported in Clarke et al. (2002), results which have led

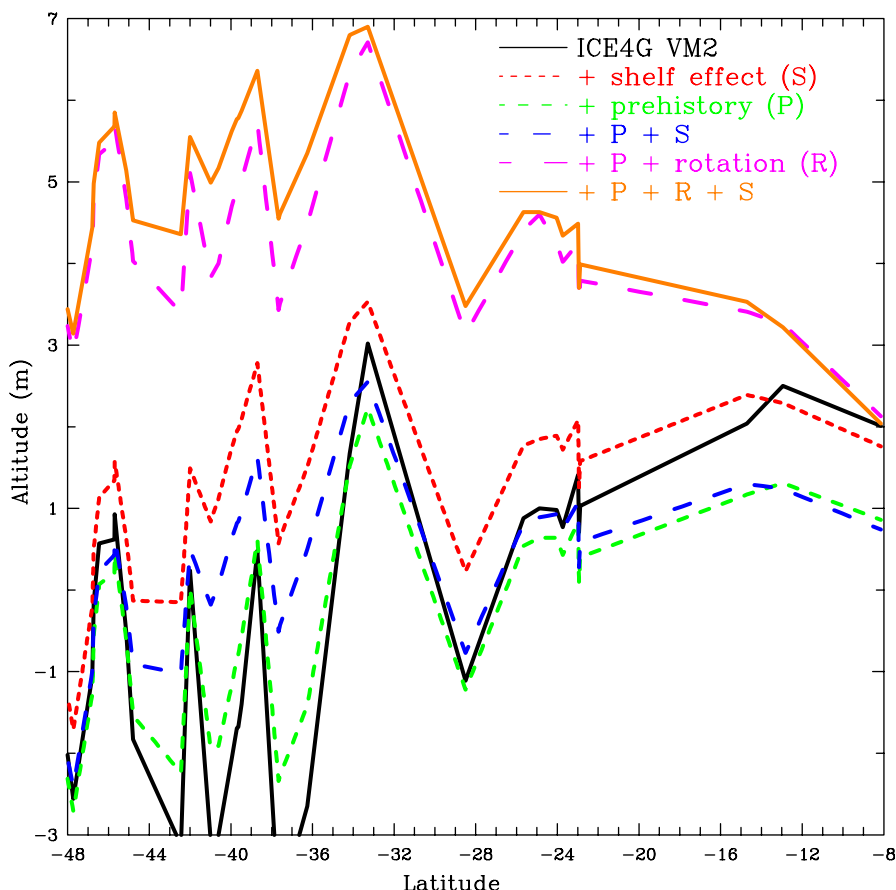


Fig. 10. Amplitude of the theoretically predicted mid-Holocene high stand of the sea as a function of latitude along the east coast of the South American continent. For the purpose of this analysis the mid-Holocene high stand has been assumed to occur, as *s* approximately the case, at an age of 6000 years before present. Results are shown on this figure for the ICE-4G (VM2) model, firstly based upon calculations that include no special effects. This result is shown as the black line. The result that includes only the “broad shelf effect” of Peltier and Drummond (2002) is shown by the dashed red line, the result that includes only the influence of the history of glaciation prior to LGM is shown as the dashed green line, whereas the result that includes both of these influences simultaneously is denoted by the dashed blue line. For all of these predictions the amplitude of the high stand is predicted to decrease as a function of increasing latitude along the coast, a result that is not in accord with the observations. When rotational feedback is included, either by adding it to the model that includes prehistory alone or by adding it to a model that includes both prehistory and the shelf effect, then the amplitude of the mid-Holocene high stand increases with increasing latitude along the coast in accord with the observations discussed in Rostami et al. (2000).

them to strongly suggest that MWP1a must have originated primarily from Antarctica. Firstly, it should be clear that a primary cause of the discrepancy between the result reported here and their result based upon the assumption of a solely Laurentide source is that when all northern hemisphere ice sheets are assumed to contribute something to MWP1a then, even on the basis of the computations reported in Clarke et al. (2002), one would expect the differential amplitude to be very much reduced. Comparing the results in their Fig. 2 labelled All-ICE3G with the result labeled Laurentia, for example, the effect is only 10%, i.e. 2.5 m. Comparing their result labeled North-ICE3G, however, which should be closest to the results for the ICE-4G model reported herein, one obtains a difference of $0.9 + 1.1$ in their terminology, or a difference of 5 m for a total MWP1a amplitude of 25 m. This is similar to but 30%

lower than the result I have reported herein for the ICE-4G and ICE-5G models. It is therefore evident, even on the basis of Clark et al.’s own calculations, that there is no logical reason to infer that a significant source of MWP1a was Antarctica, unless it can be argued that the data are sufficiently accurate to enable one to discriminate source based upon a maximum amplitude difference of 7 m.

In order to obtain the largest differential amplitude possible, one needs (according to the Clarke et al., 2002 calculations) to source all of MWP1a from the Laurentide Ice Sheet (LIS). It is implausible on physical grounds, however, that all of the meltwater involved in MWP1a could have originated from a single ice-sheet or from a single sector of a single ice-sheet. As sea level is caused to rise by the onset of rapid mass loss from a single ice-sheet, all other ice-sheets will be forced to

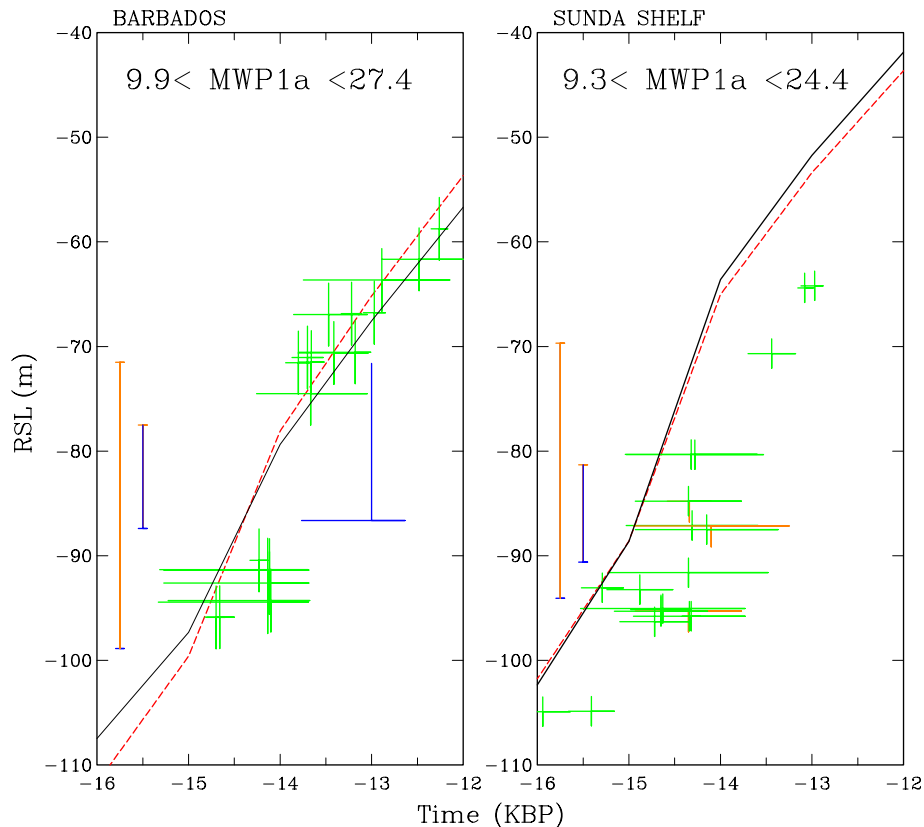


Fig. 11. Expanded scale showing the RSL observations of meltwater pulse 1-A at Barbados and the Sunda Shelf together with the predictions of model ICE-5G (VM2). The possible range of amplitude of the meltwater pulse allowed by the observations and associated error bars are shown on the individual plates of the figure.

respond as their grounding lines are floated by rising sea level. In constructing the ICE-4G model, it was assumed that the main source of MWP1a was the southern sector of the Laurentide Ice Sheet (see Fig. 5). That this geographical region of this ice complex was in fact a primary source of MWP1a appears to be well established on the basis of the analysis of Leventer et al. (1982) who reported the existence of an intense freshwater spike in $\delta^{18}\text{O}$ measured in the CaCO_3 shells of ocean plankton in the Gulf of Mexico. This is the reason why, in Fig. 5, I elected to assume that almost 50% of MWP1a was sourced in the southern sector of the LIS. Similar, essentially coincident in time, results have also been reported by Jones and Keigwin (1988) from Fram Strait, namely the existence of a freshwater spike in $\delta^{18}\text{O}$, which is expected to have been associated with the loss of mass from the Barents Sea ice complex, thus supporting the assumption in the ICE-4G reconstruction that MWP1a was sourced primarily from multiple northern hemisphere continental ice sheets.

Further indications of the primacy of an LIS source for MWP1a has recently been forthcoming on the basis of detailed reconstructions of time dependent LIS form based upon the application of modern three dimensional thermomechanical models of continental ice-sheet evolution. Analyses of post LGM LIS evolution discussed

in Tarasov and Peltier (2004), which are forced to satisfy the time evolution of the LIS margins as recently documented by Dyke et al. (2002) at high space-time resolution, demonstrate that a strong MWP1a event is required by the model in order that it fit these and other (RSL and absolute gravity) data. Seen from the perspective of Antarctica, the application of such models to the reconstruction of the post LGM history of the Antarctic Ice Sheet may similarly be seen to rule out the southern hemisphere as a significant source of MWP1a. For example, the paper of Huybrechts (2002) demonstrates that no significant mass loss from the Antarctic continent is expected until very late in the retreat of the northern hemisphere ice sheets. As Huybrechts explains, this is because the growth and decay of the Antarctic Ice Sheet is controlled entirely by sea level. It is not until sea level in the southern hemisphere has risen sufficiently that any significant mass loss can occur.

4. Discussion and conclusions

The analyses reported herein do not support the suggestion in Clarke et al. (2002), to the effect, based upon the expected differential amplitude of MWP1a at

Barbados and on the Sunda Shelf, that MWP1a must have been significantly sourced in Antarctica. Any reasonable scenario for MWP1a, in which all of the northern hemisphere ice sheets are assumed to contribute to this event, leads to the prediction of a differential amplitude of MWP1a at these locations that is not ruled out by the observations, given the error bars associated with them. Specifically the error bars associated with the *Acropora Palmata* sea level indicator employed to determine the RSL curve at Barbados are such as to imply that sea level may be as much as 5 m shallower than the depth at which the samples are found since this species of coral may live as much as 5 m below current sea level. Similarly, on the Sunda Shelf, where the RSL indicators employed to infer sea level during the MWP1a event are based upon Mangrove, these may be found as much as 2 m above sea level when the mangrove is growing. Given that the Sunda Shelf record does not in fact record the termination of the MWP1a event because of a gap in the data, it should be clear that a differential amplitude of 5–7 m is essentially undetectable by the available information. This fact is clarified in Fig. 11 where I show a blow-up of the crucial range of time at both Sunda Shelf and Barbados on which is displayed only the data from these two critical sites, together with the predictions of the previously discussed ICE-5G model, and minimum and maximum amplitudes of MWP1a allowed by the data at these locations given the error bars at each site. The data cannot constrain the amplitude at either site sufficiently accurately to rule out even the largest 7 m difference expected between the two locations. Clarke et al. (2002) apparently construe the results presented in their Fig. 3 to prove that the amplitudes at Barbados and Sunda Shelf are the same. As shown above, however, although these results do provide strong evidence that the *timing* of MWP1a at the two sites is the same, they do not provide any support for the primary argument of Clarke et al. (2002) that “fingerprinting” strongly suggests that MWP1a was significantly sourced in Antarctica.

It may nevertheless be useful to provide further comment upon the more recent work of Weaver et al. (2003) that has built upon the Clarke et al. (2002) inference of an Antarctic source for MWP1a. Although the results of the present paper do significantly undermine the logic on the basis of which this inference was made, by themselves the analyses reported herein cannot be construed to rule out the idea that some fraction of MWP1a could have originated from this southern hemisphere source. That this could not have been the sole source for MWP1a, as suggested in both Clarke et al. (2002) and assumed in the recent Weaver et al. (2003) paper is, however, clear. Firstly, there are the observations of northern hemisphere meltwater spikes of age contemporaneous with MWP1a (given the ambiguities

of age derivative of the reservoir correction etc.) mentioned previously. Equally important, however, is the fact that all reconstructions of the entire Antarctic ice sheet at LGM have led to the conclusion that the best estimate of the amount of mass lost during the glacial–interglacial transition from this region could have caused a rise in sea level of no more than approximately 14 m (see the recent papers by Huybrechts, 2002; Denton and Hughes, 2002; also Denton, personal communication 2003). There also exists considerable evidence (Huybrechts, 2002) to the effect that the collapse of the Antarctic ice sheet occurred late in the deglaciation process. In the ICE-4G reconstruction, the deglaciation of Antarctica is assumed to begin during and following the Younger-Dryas event in the northern hemisphere, an event which could have contributed to the reactivation of North Atlantic Deep Water (NADW) production in the northern hemisphere (see Fig. 2) due to the north-south “sea-saw” effect in which strengthening deep water production in one hemisphere is accompanied by weakening deepwater production in the other hemisphere (see Peltier and Solheim, 2004 for recent coupled model based illustrations of this effect). That such a late meltwater pulse did occur, is reasonably well established on the basis of the Barbados record of Fairbanks (1989 and personal communication 2003) and has been referred to in the literature as meltwater pulse 1b (MWP1b). In the ICE-4G reconstruction this Antarctica derived pulse has an important expression in the northern hemisphere, especially at sites in Scotland where the rate of rebound is sufficiently small that the arrival of the meltwater pulse induces a distinctive non-monotonic signature in the local RSL curves (Peltier, 1998; Peltier et al., 2002; Shennan et al., 2002).

None of this, of course, undermines the primary motivation of the recent analyses of Weaver et al. (2003). They are attracted to the idea of a southern hemisphere source for MWP1a as it provides a direct mechanism whereby one might be able to explain the onset of the Bölling-Allerød warm period (see Fig. 2). In their scenario, the surface freshening around Antarctica caused by MWP1a causes the production of Antarctic intermediate water to cease, and thereby activates the production of NADW which, in their scenario, is assumed to have been shut down entirely by the surface freshening associated with Heinrich event 1 (H1, see Fig. 2). It is entirely unclear, however, that the thermohaline circulation (THC) would not have spontaneously reactivated following H1. After all, each of the Heinrich events that preceded H1 was followed by a sudden warming as NADW production resumed. Previously described results of “freshwater hosing” experiments by Manabe and Stouffer (e.g. 1994, Manabe and Stouffer, 1995) show that such reactivation following the addition of a freshwater pulse to the North

Atlantic does in fact occur. It will be interesting in the future to focus more direct attention on this issue of spontaneous reactivation of the THC following a diminution of strength due to surface freshening. Simple 2-D thermohaline convection models such as that of Sakai and Peltier (1996) do spontaneously reactivate following a shutdown induced by a freshening event and these models have been employed to construct a complete northern hemisphere based scenario for both the Bölling-Allerod and Younger-Dryas events (Sakai and Peltier, 1998). We will know more concerning the feasibility of this scenario once we have tested it using fully coupled climate system models such as that recently employed in Peltier and Solheim (2004) in the context of their detailed analysis of LGM climate.

References

- Argus, D.F., Peltier, W.R., Watkins, M.M., 1999. Glacial isostatic adjustment observed using very long baseline interferometry and satellite laser ranging geodesy. *Journal of Geophysical Research* 104, 29007–29093.
- Bard, E., Hamelin, B., Fairbanks, R.G., Zindler, A., 1990. Calibration of the ^{14}C timescale over the past 30,000 years using mass spectrometric U-Th ages from Barbados corals. *Nature* 345, 405–409.
- Clark, J.A., 1976. Greenland's rapid postglacial emergence: a result of ice/water gravitational attraction. *Geology* 4, 310–312.
- Clark, J.A., Lingle, C.S., 1977. Future sea level changes due to West Antarctic ice-sheet fluctuations. *Nature* 269, 206–209.
- Clark, J.A., Farrell, W.E., Peltier, W.R., 1978. Global changes in postglacial sea level: a numerical calculation. *Quaternary Research* 9, 265–287.
- Clark, J.A., Haidle, Paul E., Cunningham, L. Nichole, 2003. Comparison of satellite altimetry to tide gauge measurement of sea level: Predictions of glacio-isostatic adjustment. *Journal of Climate*, 15, 3291–3300.
- Clarke, P.U., Mitrovica, J.X., Milne, G.A., Tamisiea, M.E., 2002. Sea level finger printing as a direct test for the source of global meltwater pulse 1a. *Science* 295, 2438–2441.
- Dahlen, F.A., 1976. The passive influence of the oceans upon the rotation of the Earth. *Geophysical Journal of the Royal Astronomical Society* 46, 363–406.
- Denton, G.H., Hughes, T., 2002. Reconstructing the Antarctic ice sheet at the Last Glacial Maximum. *Quaternary Science Reviews* 21, 193–202.
- Douglas, B.D., Peltier, W.R., 2002. The puzzle of global sea level rise. *Physics Today*, March, 35–40.
- Dyke, A.S., Andrews, J.T., Clark, P.U., England, J.M., Miller, G.M., Shaw, J., Veillette, J.J., 2002. The Laurentide and Innuitian Ice Sheets during the Last Glacial Maximum. *Quaternary Science Reviews* 21, 9–31.
- Fairbanks, R.G., 1989. A 17,000-year glacio-eustatic sea level record: Influence of glacial melting rates on the Younger-Dryas event and deep ocean circulation. *Nature* 342, 637–641.
- Farrell, W.E., Clark, J.A., 1976. On postglacial sea level. *Geophysical Journal of the Royal Astronomical Society* 46, 647–667.
- Hanebuth, T., Statteger, K., Grootes, P.M., 2000. Rapid flooding of the Sunda Shelf: a late glacial sea level record. *Science* 288, 1033–1035.
- Hemming, S.R., 2004. Heinrich events: massive Late Pleistocene detritus layers of the North Atlantic and their global climate imprint. *Reviews of Geophysics* 42.
- Huybrechts, P., 2002. Sea level changes at the LGM from ice-dynamic reconstructions of the Greenland and Antarctic ice sheets during the glacial cycles. *Quaternary Science Reviews* 21, 203–231.
- James, T.S., Lambert, A., 1993. A comparison of VLBI data with the ICE-3G glacial rebound model. *Geophysical Research Letters* 20, 871–874.
- James, T.S., Morgan, W.J., 1990. Horizontal motions due to postglacial rebound. *Geophysical Research Letters* 17, 957–960.
- Jones, G., Keigwin, L.D., 1988. Evidence from Fram Strait (78°N) for Early Deglaciation. *Nature* 336, 56–59.
- Lambert, Anthony, Courtier, Nicholas, Sasagawa, Glenn S., Kloppe, Fred, Winester, Daniel, James, Thomas S., Liard, Jacques O., 2001. New constraints on Laurentide postglacial rebound from absolute gravity measurements. *Geophysical Research Letters*, 28, 2109–2112.
- Leventer, A., et al., 1982. Dynamics of the Laurentide Ice Sheet during the Last Deglaciation: Evidence from the Gulf of Mexico. *Earth and Planetary Science Letters* 59, 11–17.
- Manabe, S., Stouffer, R.J., 1995. Simulation of abrupt climate change induced by freshwater input to the North Atlantic Ocean. *Nature* 378, 165–167.
- McManus, J.F., Francois, R., Gherardi, J.M., Keigwin, L.D., Brown-Leger, S., 2004. Collapse of Atlantic meridional circulation linked to deglacial climate changes. *Nature* 428, 834–837.
- Milne, G.A., Davis, J.L., Mitrovica, J.X., Scherneck, H.-G., Johanson, J.M., Vermeer, M., Kowula, H., 2001. Space geodetic constraints on glacial isostatic adjustment in Fennoscandia. *Science* 291, 2381–2385.
- Mitrovica, J.X., Peltier, W.R., 1991. On postglacial geoid subsidence over the equatorial oceans. *Journal of Geophysical Research* 96, 20053–20077.
- Mitrovica, J.X., Davis, J.L., Shapiro, I.I., 1994. A spectral formalism for computing three dimensional deformations due to surface loads. 2. Present-day glacial isostatic adjustment. *Journal of Geophysical Research* 99, 7075–7101.
- Mitrovica, J.X., Tamisiea, M.E., Davis, J.L., Milne, G.A., 2001. Recent mass balance of polar ice sheets inferred from patterns of global sea level change. *Nature* 409, 1026–1029.
- Peltier, W.R., 1974. The impulse response of a Maxwell Earth. *Reviews of Geophysics* 12, 649–669.
- Peltier, W.R., 1976. Glacial isostatic adjustment II: the inverse problem. *Geophysical Journal of the Royal Astronomical Society* 46, 669–706.
- Peltier, W.R., 1982. Dynamics of the ice-age Earth. *Advances in Geophysics* 24, 1–146.
- Peltier, W.R., 1994. Ice-age paleotopography. *Science* 265, 195–201.
- Peltier, W.R., 1996. Mantle viscosity and ice-age ice-sheet topography. *Science* 273, 1359–1364.
- Peltier, W.R., 1998. Postglacial variations in the level of the sea: Implications for climate dynamics and solid Earth geophysics. *Reviews of Geophysics* 36, 603–689.
- Peltier, W.R., 1999. Global sea level rise and glacial isostatic adjustment. *Global and Planetary Change* 20, 93–123.
- Peltier, W.R., 2002a. On eustatic sea level history: Last Glacial Maximum to Holocene. *Quaternary Science Reviews* 21, 377–396.
- Peltier, W.R., 2002b. Global glacial isostatic adjustment: paleogeodetic and space-geodetic tests of the ICE-4G (VM2) model. *Journal of Quaternary Science* 17, 491–510.
- Peltier, W.R., 2004. Global glacial isostasy and the surface of the ice-age Earth: The ICE-5G(VM2) model and GRACE. *Ann. Rev. Earth Planet. Sci.* 32, 111–149.
- Peltier, W.R., Andrews, J.T., 1976. Glacial isostatic adjustment, I: The forward problem. *Geophysical Journal of the Royal Astronomical Society* 46, 605–646.

- Peltier, W.R., Drummond, R., 2002. A “broad shelf-effect” in the global theory of postglacial relative sea level history”, *Geophysical Research Letters*, 29, 10-1–10-4.
- Peltier, W.R., Solheim, L.P., 2004. The climate of the Earth at Last Glacial Maximum: Statistical equilibrium state and a mode of internal variability. *Quaternary Science Reviews* 23, 335–351.
- Peltier, W.R., Farrell, W.E., Clark, J.A., 1978. Glacial isostasy and relative sea level: a global finite element model. *Tectonophysics* 50, 81–110.
- Peltier, W.R., Shennan, I., Drummond, R., Horton, B., 2002. On the glacial isostatic adjustment of the British Isles and the shallow viscoelastic structure of the Earth. *Geophysical Journal International* 148, 443–475.
- Rostami, K., Peltier, W.R., Mangini, A., 2000. Quaternary marine terraces, sea level changes and uplift history of Patagonia, Argentina: Comparisons with predictions of the ICE-4G(VM2) model of the global process of glacial isostatic adjustment. *Quaternary Science Reviews* 19, 1495–1525.
- Sakai, K., Peltier, W.R., 1996. A multibasin reduced model of the global thermohaline circulation: Paleoceanographic analysis of the origins of ice-age climate variability. *Journal of Geophysical Research* 101, 22535–22562.
- Sakai, K., Peltier, W.R., 1998. Deglaciation induced climate variability: An explicit model of the glacial–interglacial transition that simulates both the Bølling/Allerød and Younger-Dryas events. *Journal of the Meteorological Society of Japan* 76, 1029–1044.
- Shennan, I., Peltier, W.R., Drummond, R., Horton, B., 2002. Local to Global effects in postglacial sea level variations in the British Isles. *Quaternary Science Reviews* 21, 397–409.
- Tarasov, L., Peltier, W.R., 2004. A geophysically constrained large ensemble analysis of the deglacial history of the North American ice-sheet complex. *Quaternary Science Reviews* 23, 359–388.
- Weaver, A.J., Saenko, O.A., Clark, P.U., Mitrovica, J.X., 2003. Meltwater pulse 1a from Antarctica as a trigger of the Bølling-Allerød warm interval. *Science* 299, 1709–1713.
- Wu, P., Peltier, W.R., 1984. Pleistocene deglaciation and the Earth’s rotation: A new analysis. *Geophysical Journal of the Royal Astronomical Society* 76, 202–242.